Frequency-Domain Equalization of Faster-than-Nyquist Signaling

Shinya Sugiura, *Senior Member, IEEE*

***Abstract*—In this letter, motivated by the recent rediscovery of faster-than-Nyquist (FTN) signaling transmissions, we conceive a frequency-domain equalization (FDE)-assisted FTN receiver architecture, which is capable of attaining a low demodulating complexity. The proposed scheme is especially beneficial for a long channel tap FTN scenario. More specifically, in our scheme the resultant inter-symbol interference imposed by FTN signaling is approximated by a finite-tap circulant matrix structure, which allows us to employ an efficient fast Fourier transform operation and a low-complexity channel-inverse-based minimum mean-square error detection algorithm. Our simulation results demonstrate that the proposed scheme is capable of attaining a near-optimal error-rate performance without imposing any substantial demodulating complexity as well as power penalty.**

***Index Terms*—Cyclic prefix, faster-than-Nyquist signaling, fast Fourier transform, frequency-domain equalization, minimum mean-square error.**

I. Introduction

AFTER the first proposal of the faster-than-Nyquist (FTN) concept in the 1970s [1], it has recently been rediscovered as a means of boosting a transmission rate beyond that defined by the Nyquist criterion [2], without imposing any additional bandwidth expansion. In the classic band-limited scenarios employing orthogonal pulse shapes, the bound of an inter-symbol interference (ISI)-free symbol interval is given by $T_0 = 1/(2W)$[1] [3], assuming that the symbols are strictly bandlimited to W Hz. This constraint enables a simple receiver structure, relying on a matched filter and a low-complexity optimal symbol-by-symbol detection algorithm. By contrast, in the FTN signaling scheme transmitted symbol's interval T is typically set such that $T < T_0$, hence more symbols are packed in the time domain than in the conventional arrangement. Naturally, this induces unavoidable ISI effects at the receiver and imposes a higher demodulating complexity in order to eliminate ISI. However, owing to the recent advances in computing capability, FTN signaling (i.e. signaling above the Nyquist rate) has become more practical than before.

So far, a number of demodulating algorithms have been developed for the FTN-signaling receiver. For example, by considering an ISI-contaminated FTN sequence as a sort of convolutional codes, the family of Viterbi algorithms was applied in order to detect source symbols [4]; this method efficiently implements maximum-likelihood sequence estimation. Similarly, the suboptimal successive interference cancellation (SIC)-aided maximum a posteriori detector was employed in [5]. However, to the best of our knowledge, the previous demodulators developed for uncoded/coded FTN schemes were based on the time-domain equalization operation, which is not attractive in a long-tap FTN scenario due to its high demodulating complexity[2]. This limitation makes it a challenging task to achieve a moderate or high FTN's transmission rate, according to [6].

Against this background, the novel contribution of this letter is that we are the first to propose a low-complexity frequency-domain equalization (FDE) receiver structure, which can operate in the context of FTN signaling transmissions. More specifically, an addition of a short cyclic-prefix into each transmission block allows us to carry out fast Fourier transform (FFT)-based low-complexity minimum-mean square error (MMSE) demodulation at the receiver. Our proposed scheme is especially beneficial for a long-tap FTN scenario, where a delay spread associated with ISI is substantially large.

The remainder of this letter is organized as follows. Section II presents the system model of the FTN signaling transceiver and our FDE-aided receiver design. In Section III we provide the performance results of our proposed receiver and finally this letter is concluded in Section IV.

II. System Model

A. FTN Signaling

Let us consider a communication system, employing an $\mathcal{M}$-point complex-valued phase-shift keying (PSK)/quadrature amplitude modulation (QAM) scheme. At the transmitter an information symbol s_n is passed through a shaping filter $h(t)$, where n is the symbol's index. Then a block of N modulated symbols is transmitted every symbol interval $T = \alpha T_0$. Here, α is a symbol's packing ratio, which ranges from 0 to 1, where a lower α corresponds to a higher transmission rate. Then, under the assumption of additive white Gaussian noise (AWGN), the received signals may be expressed as

$$y(t) = \sqrt{E_s} \sum_n s_n g(t - nT) + \eta(t), \tag{1}$$

where we have $g(t) = \int h(\tau)h^*(\tau - t)d\tau$ and $\eta(t) = \int n(\tau)h^*(\tau - t)d\tau$. Also, $n(t)$ represents a random variable, which obeys the zero-mean complex-valued Gaussian distribution $\mathcal{CN}(0, N_0)$, having the noise variance N_0. Moreover, E_s represents the average power of transmitted symbols.

The author is with the Department of Computer and Information Sciences, Tokyo University of Agriculture and Technology, Koganei, Tokyo, 184-8588, Japan (e-mail: sugiura@ieee.org).

[1]To be specific, this bound applies to the scenario of an idealized sinc pulse shaping. The tight bound corresponding to a realistic raised cosine filter, having a roll-off factor β, is represented by $T_0 = (1+\beta)/(2W) \geq 1/(2W)$.

[2]Importantly, in the FTN signaling scheme a high transmission rate is typically achieved at the cost of an increased tap length. To be more specific, the associated complexity imposed on the receiver exponentially increases upon increasing the tap length in the classic time-domain equalization based demodulation, which is not tractable in a real-time manner for a large-block case.

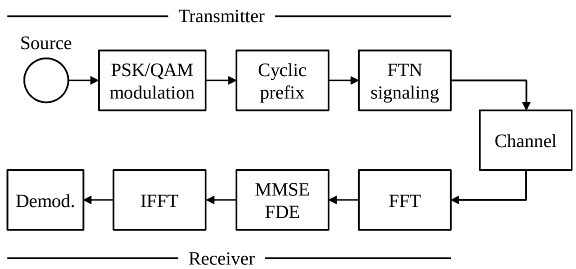

Fig. 1. The system model of our FDE-aided FTN transceiver structure.

Assuming the perfect timing synchronization between the transmitter and receiver, the kth signal sampled at the receiver may be written by

$$\begin{aligned} y_k &= y(kT) && (2)\\ &= \sqrt{E_s}\sum_n s_n g(kT-nT)+\eta(kT) && (3)\\ &= \sqrt{E_s}s_k g(0)+\sqrt{E_s}\sum_{n\neq k} s_n g(kT-nT)+\eta(kT), && (4)\end{aligned}$$

noting that the noise component $\eta(kT)$ is a zero-mean Gaussian variable, having an autocorrelation $\mathbb{E}[\eta(mT)\eta^*(nT)] = N_0 g(mT-nT)$. Furthermore, in Eq. (4) the first term represents the symbol of interest, while the second term denotes ISI. To elaborate a little further, this ISI term goes to zero for the Nyquist-rate scenario, i.e. $\alpha = 1$, hence enabling ISI-free symbol-by-symbol detection.

By contrast, the FTN signaling scheme packs more symbols within a specific block interval than its Nyquist rate counterpart. As above-mentioned, this is enabled by allowing unignorable ISI effects, which may result in an erosion of performance and an increase in demodulating complexity necessitated by equalization. As below, we incorporate the FDE concept in order to mitigate this limitation while attaining a higher normalized transmission rate of FTN signaling.

B. The Proposed FDE Aided Receiver

In our FDE-aided FTN scheme, a block-based symbol transmission is employed by adding a (2ν)-length cyclic prefix after N modulated symbols. Then, by removing both the first and the last ν-length received symbols from the $(N+2\nu)$ ones, we arrive at the N-length received signal block, which is approximated by

$$\begin{aligned} \hat{\mathbf{y}} &= [y_0, \cdots, y_{N-1}]^T \in \mathbb{C}^N \\ &= \mathbf{G}\mathbf{s}+\mathbf{n}, && (5)\end{aligned}$$

where $\mathbf{s} = [s_0, \cdots, s_{N-1}]^T \in \mathbb{C}^N$ denotes the transmitted symbol block, while $\mathbf{n} = [\eta_0, \cdots, \eta_{N-1}]^T \in \mathbb{C}^N$ represents the corresponding noise components. More specifically, the kth row of the approximated tap-coefficient matrix $\mathbf{G} \in \mathbb{R}^{N\times N}$ is defined by

$$\mathbf{g}_k = \begin{cases} [\underbrace{0,\cdots,0}_{k-1}, g(-\nu T), \cdots, g(\nu T), \underbrace{0,\cdots,0}_{N-2\nu-k}] \\ \qquad\qquad\qquad \text{for } k \leq N-2\nu \\ [g((N-k)T), \cdots, g(\nu T), \underbrace{0,\cdots 0}_{N-2\nu-1}, \\ g(-\nu T), \cdots, g((N-k-1)T)] \\ \qquad\qquad\qquad \text{for } k > N-2\nu \end{cases} \quad (6)$$

Since the matrix $\mathbf{G}$ has a circulant structure as shown in Eq. (6), we obtain the eigenvalue decomposition of $\mathbf{G} = \mathbf{Q}^T\mathbf{\Lambda}\mathbf{Q}^*$ [7], where $\mathbf{Q} \in \mathbb{C}^{N\times N}$ are the eigenvectors. With the aid of FFT, the lth-row and kth-column element of $\mathbf{Q}$ is calculated by $q_{(l,k)} = (1/\sqrt{N})\exp[-2\pi j(k-1)(l-1)/N]$. Furthermore, $\mathbf{\Lambda} \in \mathbb{R}^{N\times N}$ is the diagonal matrix, whose ith element is the associated FFT coefficient, where the calculation complexity is order $N\log N$. Although in our scheme the finite-tap approximation is assumed for the equivalent channel matrix $\mathbf{G}$ of Eq. (5), this may not be accurate depending on the packing ratio α employed. Hence, the potential modeling error $\Delta\mathbf{G} = \bar{\mathbf{G}} - \mathbf{G} \in \mathbb{R}^{N\times N}$ may result in a severe performance degradation, where $\bar{\mathbf{G}}$ represents actual infinite-ISI channels. This effect will be evaluated later in Section III.

At our FDE-aided FTN receiver, the received signals, represented in the time domain, are transformed to their frequency-domain counterparts as follows:

$$\begin{aligned} \mathbf{y}_f &\simeq \mathbf{Q}^*\hat{\mathbf{y}} && (7)\\ &= \mathbf{\Lambda}\mathbf{Q}^*\mathbf{s}+\mathbf{Q}^*\mathbf{n} && (8)\\ &= \mathbf{\Lambda}\mathbf{s}_f+\mathbf{n}_f, && (9)\end{aligned}$$

where $\mathbf{s}_f$ and $\mathbf{n}_f$ correspond to the frequency-domain signal- and noise-vectors, respectively. Then, the diagonal MMSE weights $\mathbf{W} \in \mathbb{C}^{N\times N}$ can be readily obtained according to

$$w_{(i,i)} = \lambda^*_{(i,i)}/(|\lambda_{(i,i)}|^2+N_0). \quad (10)$$

Here, $w_{(i,i)}$ and $\lambda_{(i,i)}$ represent the ith-row and ith-column elements of $\mathbf{W}$ and $\mathbf{\Lambda}$, respectively. Finally, we arrive at the time-domain symbol estimates:

$$\hat{\mathbf{s}} = \mathbf{Q}^T\mathbf{W}\mathbf{y}_f = \mathbf{Q}^T\mathbf{W}(\mathbf{\Lambda}\mathbf{s}_f+\mathbf{n}_f). \quad (11)$$

To expound a little further, the MMSE weight calculation of Eq. (10) as well as the channel inversion operation of Eq. (11) is efficiently implemented by exploiting the diagonal structure of $\mathbf{W}$.

Our FDE-aided FTN scheme's throughput is defined by

$$R = \frac{N}{N+2\nu}\cdot\frac{\log_2\mathcal{M}}{\alpha(1+\beta)}\ \text{[bits/s/Hz]}, \quad (12)$$

where the coefficient $N/(N+2\nu)$ represents a rate-loss, which arises due to the cyclic prefix insertion. Furthermore, the power penalty imposed by the cyclic prefix corresponds to $10\log_{10}[(N+2\nu)/N]$ dB. This negative effect becomes marginal for long block-size scenarios, which is similar to those of orthogonal-frequency division multiplexing (OFDM) and single-carrier (SC) modulation combined with FDE, which have been adopted in the long term evolution (LTE) standards.

C. Proposed FTN Scheme in Frequency-Selective Channels

Having introduced our FTN transceiver model under the simplified assumption of the AWGN channel, let us now carry out its extension to that applicable to frequency-selective fading environments. More specifically, we combine the above-mentioned FTN receiver with the conventional SC-FDE technique. Let us consider that the delay spread associated with frequency-selective channels spans over $LT = \alpha LT_0$ durations and that the L complex-valued tap coefficients are given by q_l $(l = 0, \cdots, L-1)$. Then, by defining the first term of Eq. (3) as $\bar{y}_k = \sqrt{E_s}\sum_{n=-\nu}^{\nu} s_n g(kT - nT)$, the received signals may be written by

$$y_k = \sum_{l=0}^{L-1} q_l \bar{y}_{k-l} + \eta(kT) \tag{13}$$

$$= \sqrt{E_s}\sum_{l=0}^{L-1}\sum_{n=-\nu}^{\nu} s_n q_l g(kT - (l+n)T) + \eta(kT). \tag{14}$$

This system model also represents a circular-matrix based linear block structure in the same manner as Eqs. (5), (6), when we have a sufficiently high ν value. Therefore the FDE-aided FTN technique derived in Section II-B is also readily applicable in this frequency-selective scenario.

Note that the effective ISI length in frequency-selective scenario is $(L-1)$ higher than that considered in the frequency-flat FTN counterpart of Section II-A. Naturally, this typically increases the demodulating complexity of the FTN signaling, hence the advantage of our low-complexity FDE-aided FTN receiver over the conventional time-domain counterpart becomes further explicit in this practical model.

D. Demodulating Complexity

As mentioned in [8], time-domain equalization is not a promising approach when ISI's delay spread is high. The complexity exponentially grows with the channel's memory size and spectral efficiency. In contrast, owing to the explicit benefit of the frequency-domain signal processing, in our scheme any substantial increase in the demodulating complexity is not imposed regardless of the tap length. In order to provide further insights, we briefly assess the proposed receiver's complexity as follows. Firstly, the received signal block's transformation from the time domain to the frequency one, represented by Eq. (7), imposes an efficient FFT operation. Next, the weight's calculations for Eq. (10) requires $4N$ real-valued multiplications. Additionally, in Eq. (11) the MMSE operation costs $2N$ real-valued multiplications as well as the inverse FFT (IFFT) operation. Hence, the total demodulating complexity per symbol [3] linearly increases upon increasing the block length N. An additional merit is that this complexity remains unaffected by the constellation size $\mathcal{M}$.

III. Simulation Results

In this section we provide our performance results in order to characterize the proposed FDE-aided FTN transceiver. We assumed that the root raised cosine filter, having a roll-off factor in the range from $\beta = 0.3$ to 0.5, was employed for $h(t)$, while considering PSK/QAM symbols, which were conveyed over the AWGN channel. The FDE-MMSE detector, formulated by Eq. (11), was used at the receiver. Furthermore, each of the transmitter and receiver was equipped with a single antenna element for the sake of simplicity. Throughout our simulations, we employed E_b/N_0 rather than E_s/N_0, where the energy loss due to the cyclic-prefix symbol was taken into account in order to implement fair performance comparisons with the conventional Nyquist-rate scenarios.

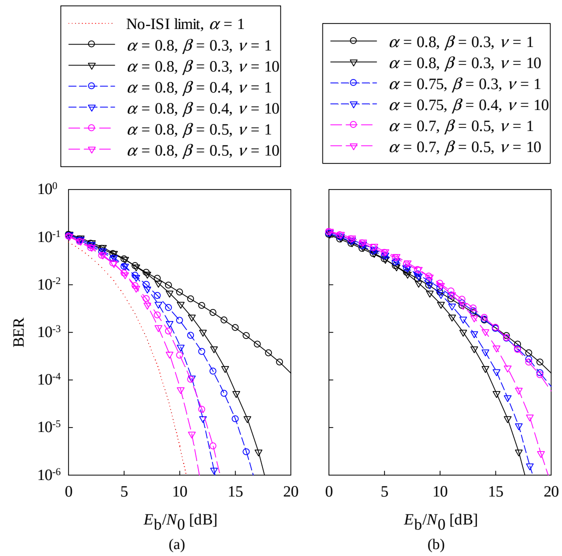

Fig. 2. Achievable BER performance of our FDE-aided FTN scheme employing BPSK modulation, where we considered the cyclic-prefix length of $\nu = 1, 10$. (a) (α, β) = $(0.8, 0.3)$, $(0.8, 0.4)$ and $(0.8, 0.5)$. (b) (α, β) = $(0.8, 0.3)$, $(0.75, 0.4)$ and $(0.7, 0.5)$.

Firstly, as shown in Fig. 2 we calculated bit-error ratio (BER) curves of our FDE-aided FTN scheme employing binary PSK (BPSK) modulation, where the cyclic-prefix length ν was set to $\nu = 1$ or 10. We note that in this scenario the relative variation of ν over the block length $N = 1,024$ remained almost constant, hence the rate-loss term of Eq. (12) is very close to unity. Moreover, in our scheme the block length N was equal to the FFT size, which was chosen as a power of two in order to allow an efficient FFT operation.

In Fig. 2(a), the symbol's packing ratio was maintained to be $\alpha = 0.8$, while varying the roll-off factor from $\beta = 0.3$ to 0.5. Also, we plotted the BER curve associated with the no-ISI scenario as a lower bound, where the optimal maximum-likelihood (ML) detector was employed. Observe in Fig. 2 that upon increasing the value of ν, the BER performance improves, where the performance difference between the proposed scheme with $(\nu, \beta) = (10, 0.5)$ and the no-ISI limit was as low as 1 dB. We note that this was achieved at the additional cost of expanded bandwidth. Furthermore, in Fig. 2(b) we also compared the BER performance of additional FDE-aided FTN scenarios, which have a similar bandwidth efficiency R. More specifically, we considered those of (α, β) = $(0.8, 0.3)$, $(0.75, 0.4)$ and $(0.7, 0.5)$. As shown in Fig. 2(b)

[3]Here, the complexity is evaluated in terms of the number of real-valued multiplications, where a single complex-valued multiplication corresponds to four real-valued ones [9].

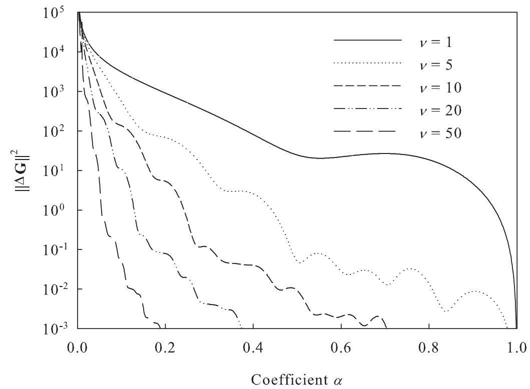

Fig. 3. Effects of the values ν and α on the modeling error of an equivalent ISI-contaminated channels $\|\Delta\mathbf{G}\|^2$, where we considered the block size of $N = 1,024$ and the roll-off factor of $\beta = 0.4$.

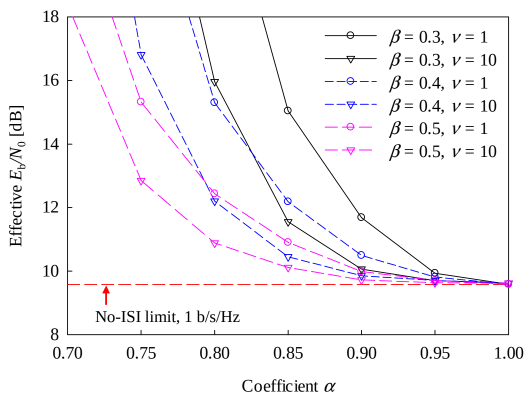

Fig. 4. Effective E_b/N_0 recorded for BER $= 10^{-5}$, where the symbol's packing ratio α was varied from 0.7 to 1.0 and the cyclic-prefix length was given by $\nu = 1$ and 10 in our FDE-aided FTN scheme employing BPSK modulation. The no-ISI limit, associated with $\alpha = 1$, was also plotted as the lower bound.

the results exhibited some performance variations, which were not substantial in comparison to those of Fig. 2(a). Therefore, given a target bandwidth efficiency R and a cyclic-prefix size 2ν, a parameter set (α, β) may be appropriately optimized for a further slight performance improvement.

Next, in Figs. 3 and 4, we investigated the effects of α and ν on the achievable BER performance. Here, we also assumed the employment of BPSK modulation. Specifically, in Fig. 3, the square error $\|\Delta\mathbf{G}\|^2$ imposed by the channel's finite-tap approximation was plotted, where we considered $\nu = 1, 5, 10, 20, 50$ and $\beta = 0.4$, while varying α from 0 to 1. It can be seen in Fig 3 that upon decreasing the value of α, the modeling error $\|\Delta\mathbf{G}\|^2$ associated with finite-tap approximation of Eq. (6) became higher. This was due to the fact that the cyclic prefix was lower than the effective delay spread. Hence, the size of cyclic prefix ν has to be sufficiently high in order to eliminate the ISI effect.

Similarly, in Fig. 4 we plotted the effective E_b/N_0 value, which was recorded for BER = 10^{-5}, where the value of α was varied from 0.7 to 1 with a step size of 0.05. Observe in the high-α regime of Fig. 4 that any significant performance penalty was imposed in our scheme. By contrast, the lower α value lead to the higher effective E_b/N_0, as predicted from the Mazo limit [1] as well as from the high interference effect shown in Fig. 3. In order to eliminate the performance difference imposed between the Nyquist-rate scenario and our FDE-aided FTN one having a moderate α value, the employment of powerful channel-encoding schemes, such as turbo and low-density parity check codes, is typically required, as mentioned in [4], [10]. Also in such an iteratively-decoded FTN arrangement, the low receiver complexity of our FDE-based approach is promising.

As mentioned in [8], the FDE operation typically exhibits an order lower complexity than its time-domain equalization counterpart when the tap length is higher than 50. The same holds true for the FTN signaling scheme. Hence, the proposed scheme is especially useful for a long channel tap scenario.

IV. Conclusions

In this letter, we have proposed the FDE-aided FTN signaling receiver, which is capable of attaining a low-complexity detection by relying on a diagonal MMSE criterion and an efficient FFT operation. This is especially beneficial for a long-tap FTN scenario, where the effective tap-length of ISI-contaminated channels is significantly high. Our simulation results demonstrate that the proposed scheme is capable of attaining a near-optimal error-rate performance without imposing any substantial demodulating complexity as well as power penalty. Lastly, the proposed scheme will also be beneficial for the FTN scheme's practical use in optical links [11].

References

[1] J. E. Mazo, "Faster-than-Nyquist signaling," *Bell System Technical Journal*, vol. 54, no. 8, pp. 1451–1462, 1975.
[2] J. B. Anderson, F. Rusek, and V. Owall, "Faster than Nyquist signaling," *Proceedings of the IEEE*, vol. 101, no. 8, pp. 1817–1830, Aug. 2013.
[3] J. G. Proakis, *Digital Communications*, 5th ed. McGraw-Hill, New York, 2008.
[4] A. D. Liveris and C. N. Georghiades, "Exploiting faster-than-Nyquist signaling," *IEEE Transactions on Communications*, vol. 51, no. 9, pp. 1502–1511, 2003.
[5] F. Rusek and J. Anderson, "Multistream faster than Nyquist signaling," *IEEE Transactions on Communications*, vol. 57, no. 5, pp. 1329–1340, May 2009.
[6] Y. G. Yoo and J. H. Cho, "Asymptotic optimality of binary faster-than-Nyquist signaling," *IEEE Communications Letters*, vol. 14, no. 9, pp. 788–790, Sep. 2010.
[7] N. Al-Dhahir, "Single-carrier frequency-domain equalization for space-time block-coded transmissions over frequency-selective fading channels," *IEEE Communications Letters*, vol. 5, no. 7, pp. 304–306, Jul. 2001.
[8] D. Falconer, S. Ariyavisitakul, A. Benyamin-Seeyar, and B. Eidson, "Frequency domain equalization for single-carrier broadband wireless systems," *IEEE Communications Magazine*, vol. 40, no. 4, pp. 58–66, Apr. 2002.
[9] S. Sugiura, S. Chen, and L. Hanzo, "MIMO-aided near-capacity turbo transceivers: Taxonomy and performance versus complexity," *IEEE Communications Surveys & Tutorials*, vol. 14, no. 2, pp. 421–442, Second Quarter, 2012.
[10] D. Dasalukunte, F. Rusek, and V. Owall, "An iterative decoder for multicarrier faster-than-Nyquist signaling systems," in *IEEE International Conference on Communications (ICC)*, Cape Town, South Africa, 2010, pp. 1–5.
[11] G. Colavolpe, T. Foggi, A. Modenini, and A. Piemontese, "Faster-than-Nyquist and beyond: How to improve spectral efficiency by accepting interference," *Optics Express*, vol. 19, no. 27, pp. 26 600–26 609, Dec. 2011.